

Semantic Segmentation-Based Study of Solar Panel Footprints in Hong Kong

NG Tsz kin and NG Nok Hang, Hong Kong, China

Key words: Remote Sensing; Optical Remote Sensing, Aerial Image, Orthophoto; True Orthophoto; Convolutional Neural Network; U-Net; Deep Learning; Semantic Segmentation; Computer Vision; Solar Panel

SUMMARY

The rapid growth of human activities has resulted in an increased demand for energy and raised concerns about the environment, necessitating the exploration of sustainable energy sources. Solar energy, in particular, has gained significant attention due to its renewable and clean nature. In Hong Kong, there is a growing adoption of solar panels driven by their renewable and clean characteristics. The Government of the Hong Kong Special Administrative Region (HKSAR) has also introduced the Feed-in-Tariff (FiT) Scheme and "Solar Harvest" to encourage private sector involvement in small-scale distributed renewable energy generation. As a result, the number of solar panels in Hong Kong has significantly increased in recent years.

Earth observation data is commonly used to identify land features such as solar panels. However, the quality of optical imagery data can vary due to different image acquisition conditions, such as atmospheric conditions, flying height, and ground shadows. In this study, very high-resolution aerial orthophotos were utilized to label large amounts of imagery data for solar panels. The U-Net architecture and post-processing techniques were then employed to identify the location of solar panels and overcome the radiometric variation in the images, thereby mapping the solar panel footprint across the entire Hong Kong region.

This study demonstrated that the developed workflow successfully adapted to varying radiometric conditions and effectively identified the footprint of solar panels, with a minimum mapping unit of one solar panel size. Solar panels are commonly found on the rooftops of village houses, industrial buildings, schools, as well as floating within water ponds and on the roofs of bus vehicles in Hong Kong. An independent check revealed that the Intersection over Union (IoU) and F1 Score of the identified solar panels were 0.90 and 0.95, respectively, further confirming the feasibility of the workflow.

The study identified the distribution of solar panels within the Hong Kong area, highlighting their prevalence on specific rooftops and buildings. This contributes to the development of a hierarchical land cover map and enables the identification of newly added or removed solar panels by comparing different years of data capture. Furthermore, the study provides spatial information on existing solar panels to policymakers, facilitating informed decisions regarding sustainable energy infrastructure and ultimately supporting Hong Kong in achieving the United Nations' Sustainable Development Goals.

Semantic Segmentation-Based Study of Solar Panel Footprints in Hong Kong

NG Tsz kin and NG Nok Hang, Hong Kong, China

1. INTRODUCTION

The rapid expansion of human activities has resulted in an escalating demand for energy and growing environmental concerns. As a result, the exploration of sustainable energy sources has become imperative. Solar energy, in particular, has garnered significant attention due to its renewable and environmentally friendly characteristics. The installation of solar panels offers a practical solution to reduce reliance on fossil fuels and mitigate the emission of greenhouse gases. Recognizing the potential of solar power, the Government of the Hong Kong Special Administrative Region (HKSAR) has published guidance notes [4] to encourage the private sector's involvement in small-scale distributed renewable energy generation. With the increasing adoption of solar panels in Hong Kong [11], it is crucial to gain insights into their distribution and quantify their prevalence through mapping. Leveraging Earth Observation data and advanced technologies, the identification of the solar panel footprint can enhance various services, including policy planning, resource allocation, and monitoring progress towards sustainable energy objectives. This study, therefore, developed methodologies capable of accurately counting and mapping the solar panel footprint.

2. RELATED WORKS

Solar panel footprint detection is not a new topic. During the research stage, numerous articles on solar panel detection or related subjects were thoroughly examined. Wang et al. (2023) suggested the use of a semantic segmentation model to extract the footprint and attributes of large-scale PV systems from higher-resolution images, which is limited in the currently available public datasets and do not provide detailed footprints for PV panels or attributes such as the location, quantity, or area of these panels[14]. Kausika, Nijmeijer, Reimerink, Brouwer, and Liem (2021) demonstrated that the National Mapping Agency of the Netherlands implemented a comprehensive solution, encompassing image capture, orthophoto production, labeling, model training and prediction, and accuracy evaluation. This approach was utilized to create a nationwide database of solar panel installations on buildings, using a deep learning approach and high-resolution aerial images[7]. The approach proposed by Wu and Biljecki (2021) was considered to demonstrate the trained model's ability in new areas without relying on training data, thereby facilitating the extension of the work to include new cities[16].

Many studies have emerged in recent years to address this task. Wang et al. (2023) proposed five models from the field of semantic segmentation and compared their performance with their proposed PVNet, using the same parameter settings and loss functions[14]. Chen, Kang, Sun, Wu, and Zhang (2022) compared the performance of three machine learning algorithms:

XGBoost, Random Forest (RF), and Support Vector Machine (SVM). They combined original spectral features, PV extraction indexes, and terrain features to accurately identify PV plants [1]. Wani and Mujtaba (2021) proposed the use of a combined MobileNet and U-Net architecture to identify solar panels from very high-resolution satellite images[15]. Li et al. (2021) suggested that the characteristics of PV segmentation as a computer vision issue, revealing a series of challenges, giving a series of targeted better using recommendations for PV segmentation[9].

Deep learning requires a large number of training samples. Chen, Kang, Sun, Wu, and Zhang (2022) implemented a two-step labeling process. They selected two experienced annotators to label the samples using Google Earth Pro, and then cross-validated the labeled samples. Any unclear points were discussed with independent third annotators until a consensus was reached regarding the outcomes of the sample points[1]. Wu and Biljecki (2021) considered randomly labeling the building rooftops to ensure sufficient representation of the selected cities[16].

Accuracy assessment is always important in evaluating the success of a task. Wani and Mujtaba (2021) suggested that the performance of semantic segmentation for a specific object should not only be evaluated based on its classification accuracy and shape of the predicted object, but also consider factors such as computational efficiency, training time, and the number of parameters required[15]. Wu and Biljecki (2021) proposed a two post-processing approach to reduce false positives, including simplifying the polygon by reducing the number of shapes and denoising the prediction results to remove speckles[16].

3. DATA PREPARATION

3.1 Study Area

This study mainly focused on the land and coastal area within Hong Kong, subject to the availability of data source.

3.2 Data Source

This study applied the aerial orthophoto, named DSM-Orthophoto as the primary data source to annotate training dataset, train the model, and identified the solar panel footprints. DSM-Orthophoto is a true orthophoto product generated by the Survey and Mapping Office (SMO), Lands Department of the Government of HKSAR. A large format UltraCam Eagle 4.1 camera [10] is mounted on a Government fixed wing aircraft for the aerial survey taken at a flying height of about 6,900 ft above MSL, which captured the entire Hong Kong area annually with an end-lap of 80% and a side-lap of 60%. The batch of aerial photos were then used to produce the true orthophoto and digital surface model (DSM) with a ground sampling distance (GSD) of no better than 4 cm. Normally, this true orthophoto rectifies all physical features, including buildings and elevated roads, through the utilization of the true orthophoto processing method. Similar to the aerial photo capture, this true orthophoto consists of four bands (named Red,

Green, Blue and NIR), and are supplied on tile basis. Each tile is equivalent to the coverage of the 1:1000 Topographic map tile[8], mapping the real world in 750 m x 600 m extent.

Since the production of DSM-Orthophoto is a semi-automatic workflow, image distortions might appear at some areas of the DSM-Orthophoto such as area around tall structures, shadows, narrow gaps, features mixed with vegetation and water bodies, concluding as artifacts of orthophoto. Areas without any orthophoto (no data) within a tile are shown in white in that tile. The horizontal accuracy of a DSM-Orthophoto with 5 cm resolution achieved 0.3 m or better.

Between 1 February and 2 June 2023, 3240 tiles of DSM-Orthophoto (Table 1) in GeoTIFF format including a TFW World file with geo-referencing data in Hong Kong 1980 Grid were used. They covered nearly the whole extent of Hong Kong (Figure 1). In this study, only RGB layers of DSM-Orthophoto were applied and no additional tiling cut had been made.

Table 1: The number of available tiles across each district in Hong Kong

| District | No. of Tiles | District | No. of Tiles |
|----------------|--------------|--------------------------------|--------------|
| Hong Kong (HK) | 254 | Sha Tin (ST) | 157 |
| Island (Is) | 690 | Tai Po (TP) | 428 |
| Kowloon (K) | 126 | Tsuen Wan & Kwai Tsing (TW&KT) | 200 |
| North (N) | 348 | Tuen Mun (TM) | 235 |
| Sai Kung (SK) | 469 | Yuen Long (YL) | 333 |

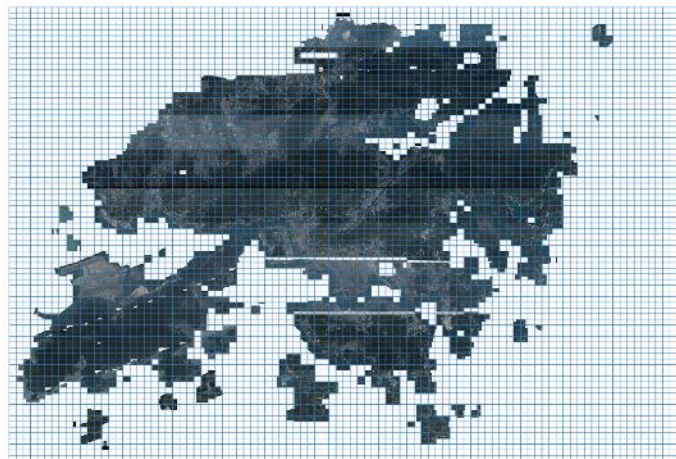
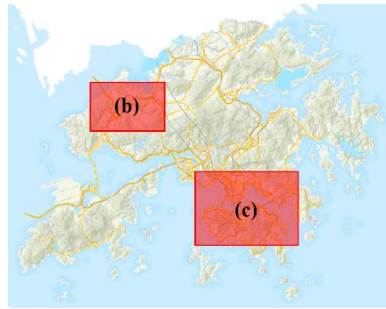


Figure 1: The footprint of DSM-Orthophoto used in this study

3.3 Annotation

In the feature extraction of solar panels, supervised classification was applied, which required a large amount of ground truth data. To ensure sufficient amount of solar panel being labelled, 26 DSM-Orthophotos, captured in 2022 and in B1000 tiles extent were annotated, of which 21 tiles are situated in the Yuen Long District and 5 tiles are located in the Hong Kong Island or Kowloon region. The annotation process consisted of two steps.



(a) Location Map of 2(b) and 2(c)



(b) Yuen Long



(c) HK Island and Kowloon

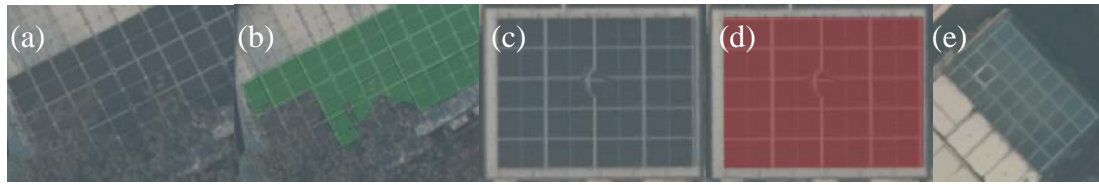
Figure 2: The Distribution of Annotated Tiles

3.3.1 Annotation Method

First, each annotator was assigned a batch of orthophotos, overlaying them and digitizing each solar panel individually using GIS software in shapefile format. Solar panels that were packed closely, within an euclidean distance of less than 1 meter in the real world from each other, were digitized as a single polygon. To ensure consistent digitization, an independent checker who did not participate in the initial annotation process conducted periodic reviews and cross-checked at least 10% of the annotated results. Any discrepancies or errors found in the annotations among annotators were required to be revised. In cases where there were marginal cases, annotators and checkers engaged in group discussions to reach a consensus among themselves, aiming to obtain consistent annotations across the team.

3.3.2 Challenges faced in Annotation

During the annotation, three types of non-typical cases were observed which induced the difficulties in annotation. They arose from the limitation or artifacts of data source, and the realistic situation of solar panel installation in Hong Kong, including feature blockage (Figure 3a and 3b), feature distortion (Figure 3c and 3d), and feature confusion (Figure 3e). However, the study encountered a class imbalance problem, which means that one class (e.g., the target) may have significantly fewer samples than the other (e.g., the background). To reduce the effect of class imbalance problem, the annotated image being splitted which contains at least one pixel of solar panel would be considered as valid annotation dataset.



(a) Part of the solar panels being blocked by vegetation; (b) The annotated result of (a) case; (c) Part of solar panel being distorted; (d) The annotated result of (c) case; (e) Example of glass roof being misannotated as solar panel (From left to right)

Figure 3: The Examples of 3 Non-typical Cases

3.3.3 Number of Annotated Files

In total, it contributed a dataset of 1805 images with dimensions of 512 pixel x 512 pixel, containing whole or part of solar panels, and was used for model development. 80% of these images (1444 images) were used to train the model, while the remaining 20% (361 images) were used to independently evaluate the model's performance.

4. METHODOLOGY

4.1 Overview

In this study, a designed workflow is derived (Figure 4), consisting of several crucial steps and aimed at training a model to accurately identify solar panel footprints. The first step involved training a U-Net model using a batch of orthophotos that had been annotated with solar panel labels. If the model's prediction results were not deemed satisfactory, fine-tuning of hyperparameters would be conducted. An independent accuracy check was performed after each training iteration to validate the model's performance. Once the model had been trained and its accuracy had been verified, the workflow moved to the mass-production stage for predicting solar panel footprints across the entire territory of Hong Kong.

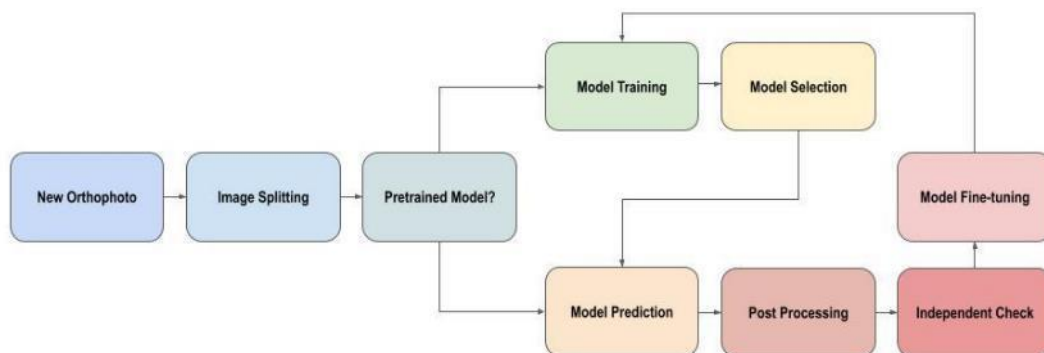


Figure 4: Workflow of Semantic Segmentation of Solar Panel Footprint

4.2 Model Architecture

This study used U-Net encoder and decoder architecture[12]. This architecture was employed to train the model and achieve binary segmentation, where each pixel was assigned a label indicating whether it belonged to the target class (labeled as 1) or the background (labeled as 0). The encoder part consisted of four blocks. Each block applied two 3x3 convolutions followed by a ReLU activation function for features extraction and a 2x2 max pooling operation to downsample the input. The filter number of the convolution was doubled each time after the downsampling, increased from 64 all the way to 1024 across four blocks. A Bridge block, comprising merely two convolutions-ReLU operations, was attached to the end of the encoder and connected to the head of the decoder. In the decoder part, an identical number of blocks as the encoder was used. In order to upsample the feature map back to the original input size to form a segmentation mask, each block needed to perform a 2x2 transposed convolution. For a more accurate upsampling result, the output of the transposed convolution in each decoder block needed to be concatenated with the corresponding feature map from the encoder block so that the positional information could be transferred to the decoder. After that, two 3x3 convolutions and a ReLU were applied. The filter number of convolution in each block was half of the previous block which was the opposite of the setting in the encoder. The final layer was a 1x1 convolution aimed at mapping the feature vector to the output number of the classes, which in this study were the solar panel and background. A sigmoid activation function was added at the end to generate per-pixel probabilities belonging to the target class (Figure 5). The code implementation of this project referenced the Zhixuhao (2019) GitHub repository[18].

In addition to the architecture, the model's predictions were required to be applicable to DSM-Orthophoto images captured at different points in time. These images exhibited variations in local atmospheric and radiometric conditions, including differences in brightness, haze, and shadow distribution. To address this, various pre-processing techniques were attempted. Image normalization using histogram equalization or expert decision-making was explored. However, these approaches did not yield effective results and were not applicable to all available images. The study also considered using overlapping of 50% end-lap and 50% side-lap, as well as rotation at eight angles for the DSM-Orthophoto images. It aimed at increasing the amount of annotated data. However, it was found that these approaches would significantly increase data processing time without greatly enhancing the result. Hence, the above augmentation was not ultimately applied. To further enhance the prediction accuracy of the model, the variety and quantity of annotated images were increased through augmentation techniques. Automatic augmentation was implemented, which involved applying various transformations to each annotated image, including 90-degree rotation, horizontal flipping, vertical flipping, brightness variation, contrast variation, and color hue variation with a random rate.

During the training process, the number of epochs was set to 100 with an early stop patience of 10 epochs. This meant that the number of training samples transformed for model training would not exceed 144,400 ($1805 \times 0.8 \times 100$), while the model used for independent evaluation would be trained with 361 samples (1805×0.2).

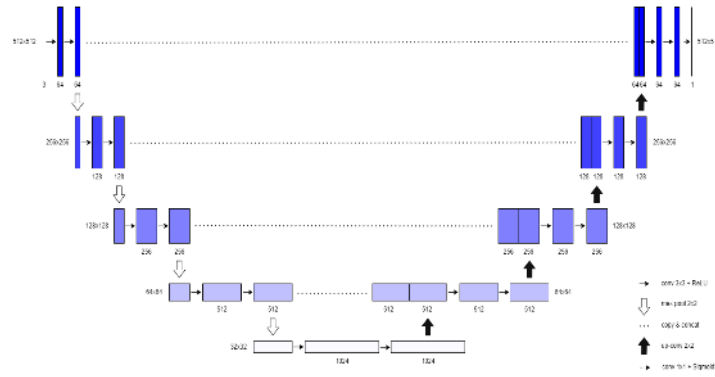


Figure 5: Architecture and Parameters in each Layer

4.3 Post-processing

During the model prediction process, each pixel was assigned a probability value ranging from 0 to 1, indicating the likelihood of being identified as a solar panel. To filter out pixels with low probability, threshold value of 0.5 was used. Additionally, since each solar panel system typically had a regular shape, the area-to-perimeter ratio and vertex-to-area ratio were applied to ensure that the solar panel predictions aligned with real-world situations. To remove salt and pepper noise, all pixels with a prediction value less than the area of one 60-cell module of solar panel[5] i.e. 1.6 sq. m were filtered out. Last but not least, hole filling was applied on post-processed polygons for the sake of better presentation of solar panel footprint, by using "union and dissolve" in GIS software. Two examples were shown in Figure 6.

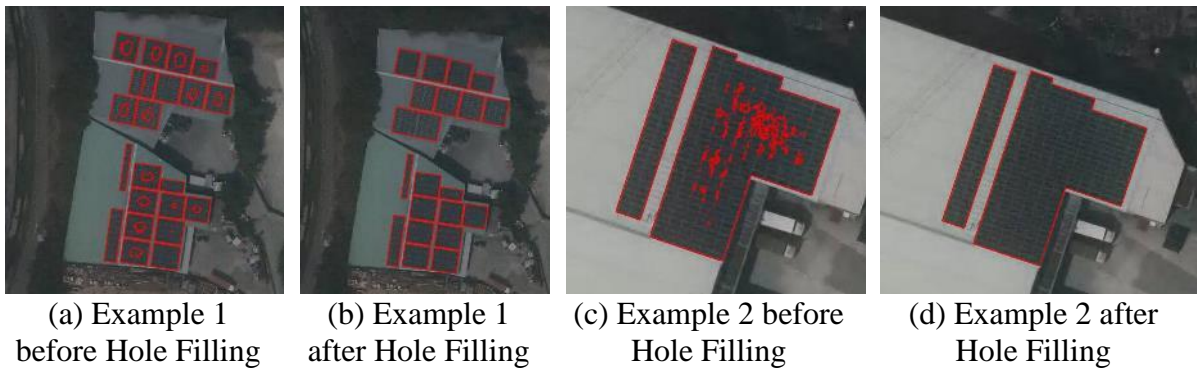


Figure 6: 2 Examples of Hole Filling

5. RESULTS AND DISCUSSION

5.1 Presentation

The solar panel prediction and post-processing step were conducted for the entire territory of Hong Kong using the aforementioned DSM-Orthophoto in 2023 in B1000 tile. Solar panels were found on roof tops of industrial buildings, buses, schools, small houses, high rise residential buildings, temporary structures, yatangs and floating photovoltaic (FPV) systems

on fish ponds and reservoirs (Figure 7). Under most circumstances, the shapes and footprints of the solar panels were accurately mapped. Considering the resolution of images, the quality of the labeling, and the post-processing work, the Minimum Mapping Unit (MMU) of this segmentation result was as precise as one typical size of 60-cell solar panel module i.e. 1.6 sq. m. The solar panel results were quantified and summarized in the following table (Table 2). According to the heatmap showing the distribution in Hong Kong (Figure 8). Yuen Long has the denser distribution of solar panel across the districts.

Also, the results of solar panel showed that some glass roofs on building tops and covered walkways, or any objects which have similar size, shape, and frame to solar panels, were incorrectly predicted. Additionally, areas under dark shadows could not be predicted.

Table 2: The Summary of Solar Panel Results

| District | No. of DSM-Orthophoto in B1000 Tile | No. of Machine-Predicted Polygons | No. of Post-Processed Polygons | Fill hole Area (sq. m.) | No. of Solar Panels Module |
|----------|-------------------------------------|-----------------------------------|--------------------------------|-------------------------|----------------------------|
| HK | 254 | 15,717 | 4,410 | 65,926 | 41,204 |
| Is | 690 | 13,818 | 5,145 | 104,728 | 65,455 |
| K | 126 | 22,634 | 7,627 | 144,622 | 90,389 |
| N | 348 | 12,559 | 5,292 | 161,498 | 100,936 |
| SK | 469 | 12,715 | 5,948 | 122,020 | 76,262 |
| ST | 157 | 18,216 | 4,821 | 92,898 | 58,061 |
| TM | 235 | 14,130 | 5,671 | 135,898 | 84,936 |
| TP | 428 | 18,651 | 8,639 | 185,254 | 115,784 |
| TW&KT | 200 | 12,899 | 4,741 | 117,620 | 73,513 |
| YL | 333 | 39,477 | 17,930 | 512,758 | 320,474 |
| Total | 3240 | 180,816 | 70,224 | 1,643,221 | 1,027,013 |



(a) Roof Tops of Industrial Buildings



(b) Buses in Bus Depot



(c) Roof Tops of School



(d) Roof Tops of Small Houses



(e) Roof Tops of High Rise Residential Buildings



(f) Roof Tops of Temporary Structures

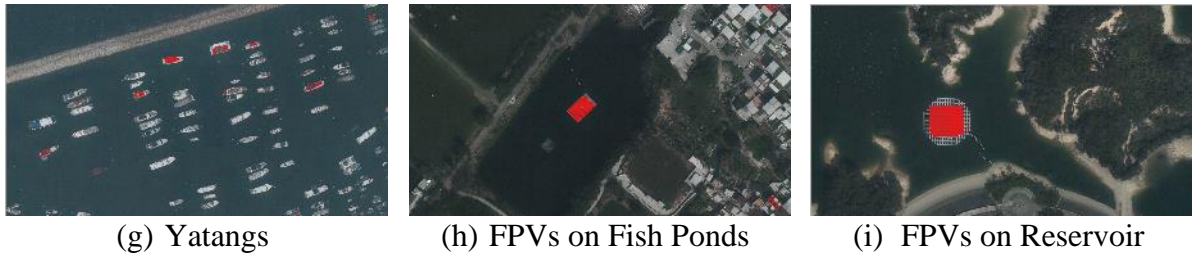


Figure 7: Examples of Identified Solar Panels

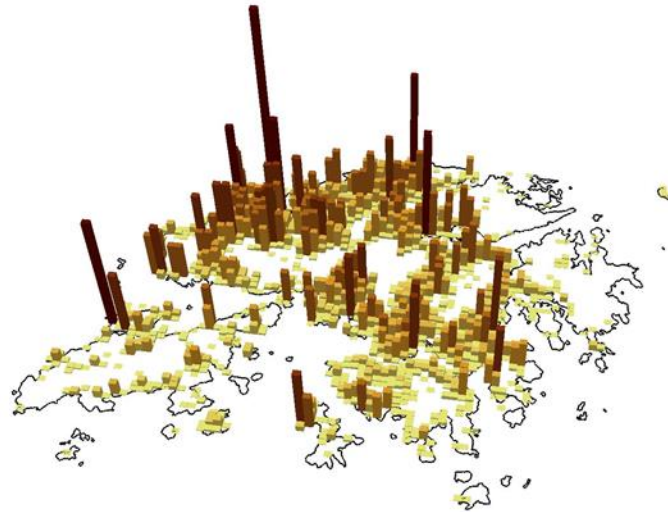


Figure 8: The Heat Map of Solar Panel Footprint in Hong Kong

5.2 Accuracy Assessment

The performance of this workflow required evaluation. It was divided into two parts: an accuracy check by an annotation dataset in 5.2.1 and an accuracy check by 10% sampling in 5.2.2.

5.2.1 Accuracy Check by Annotation Dataset

Since the annotated images used for model development were split into training and validation datasets, the validation dataset was used to validate the prediction performance by comparing it with the model's prediction. It was reflected by F1 score and Intersection of Union (IoU). The respective accuracies are presented below (Table 3).

Table 3: Evaluation Matrix of Annotation Dataset

| Evaluation Dataset | | F1 Score | IoU |
|--------------------|----------------------|----------|-------|
| Training | 80% Annotated Images | 90.5% | 80.5% |
| Validation | 20% Annotated Images | 88.1% | 98.0% |

5.2.2 Advanced Accuracy Check by Sampling

To further evaluate the performance, an independent dataset named the Manual Checked Dataset was generated by the model initially and then underwent manual checking via visual inspection one by one. This dataset covered the Yuen Long District with 333 tiles (about 10% of the dataset) and was used to evaluate the Post-processed Dataset (Table 4). The F1 score and IoU were calculated as 0.95 and 0.90, respectively. Through manual screening, the areas of predicted polygons was slightly different from the manually checked ones. The reasons for the differences are also summarized in Table 5.

Table 4: Evaluation Matrix of the Post-processed Dataset against the Manual Checked Dataset

| | Solar Panel | Non-Solar Panel |
|--|-------------|-----------------|
| Area of TP Polygon (sq. m) | 511,950 | 147,034,601 |
| Area of FP Polygon (sq. m) | 20,103 | 37,768 |
| Area of FN Polygon (sq. m) | 37,768 | 20,103 |
| Area of Manual Checked Dataset(sq. m) | 549,717 | 147,054,704 |
| Area of Post-processed Dataset (sq. m) | 532,052 | 147,072,369 |
| Precision | 0.96 | >0.99 |
| Recall | 0.93 | >0.99 |
| F1 Score | 0.95 | >0.99 |
| IoU | 0.90 | >0.99 |
| Mean F1 Score | 0.97 | |
| Mean IoU | 0.95 | |
| Weighted F1 Score | >0.99 | |
| Weighted IoU | >0.99 | |

Table 5: Quality of the Post-processed Dataset against the Manual Checked Dataset

| Case | No. of Polygon | % | Area | % | |
|-------|----------------------|--------|------|---------|-----|
| 1 | Correct Prediction | 9,248 | 82 | 509,132 | 94 |
| 2 | Over Prediction | 32 | <1 | 1,286 | <1 |
| 3 | Lower Prediction | 109 | <1 | 2,810 | 1 |
| 4 | Incorrect Prediction | 1,419 | 13 | 18,824 | 3 |
| 5 | Unpredictable Object | 496 | 4 | 7,808 | 1 |
| Total | | 11,304 | 100 | 539,860 | 100 |

5.3 Resources Used

During the training and prediction process, two powerful workstations with high-performance GPU and CPU were deployed. Depending on the size of the dataset, sufficient RAM was also crucial for handling the large amount of data involved during training. The computer specifications, model training time, and model prediction time for predicting solar panels using the aforementioned DSM-Orthophotos are summarized in Table 6 below. Adequate storage space was necessary to store the source of images, datasets, model checkpoints, and

intermediate results during training. In our case, 2,746 GB memory was used and stored in a network-attached storage (NAS), but a 1.5x to 2x storage buffer should be reserved.

In the realm of this study, it was crucial to have the appropriate tools installed on the workstation including some deep learning frameworks like TensorFlow, PyTorch, and Keras, as well as the necessary software libraries and drivers to effectively utilize the GPU. To facilitate model development, Jupyter Notebook was used for data cleansing, the creation and sharing of documents containing code, computation output, data visualizations, and procedural documentation. For data post-processing and accuracy checking, GIS software like ESRI ArcGIS Pro and QGIS proved invaluable in handling tasks such as GIS operations, data cleansing and format conversation.

Table 6: Computer Resources

| | Computer 1 | Computer 2 | Total |
|------------------------|--|---|----------|
| Computer Specification | CPU: Intel(R) Xeon(R) Platinum 8260 CPU @ 2.40GHz 2.39 GHz (2 processors); RAM: 512 GB; GPU: RTX6000 | CPU: AMD Ryzen Threadripper PRO 3975WX 32-Cores 3.50 GHz; RAM: 512 GB; GPU: RTX8000 | N.A. |
| Model Training Time | About 45 hours (about 22 seconds per iteration) | N.A. | 45 hours |
| Prediction Time | 50 mins per B1000 tile (for ST district only) | 8 mins per B1000 tile (for the rest of Hong Kong) | 23 days |

6. APPLICATION

6.1 Land Cover Map and Change Detection

Land cover is an abstraction of the physical and biophysical cover on the earth’s surface including both natural and artificial surfaces[3]. One essential application of semantic segmentation-based analysis is the integration of solar panel footprints into the existing Land Cover Map of Hong Kong. The Land Cover Map is a hierarchical classification system developed by our office, which provides a comprehensive and standardized nomenclature for categorizing different land cover features types. Solar panels represent a distinct class within the Level 2 classification hierarchy of the Land Cover Map. This classification offers significant support for change detection applications in the context of solar panel footprints in Hong Kong. By periodically analyzing the imagery data using the approach described above, the changes in the spatial distribution of solar panels can be effectively monitored. For example, solar panel installations were destroyed after the typhoon[13]. This information can be used as one of the indicators to assess the effectiveness of solar energy policies, to evaluate the impact of incentive schemes, and to identify areas with rapid adoption or potential underutilization of solar energy.

6.2 Identification of Supply and Demand of Solar Energy

By utilizing the existing building polygon data from the Common Spatial Data Infrastructure (CSDI) Data, which is one of the Framework Spatial Data Themes (FSDT)[2] of Hong Kong's CSDI, it is possible to identify the current density of solar panel installations on building rooftops within the Hong Kong territory. This information allows for the prediction of the current number of solar panel installations and their distribution across different types of buildings, such as high rise buildings, small houses and school rooftops. Furthermore, solar panel installations in Hong Kong can comprise different types of PV systems[6]. By integrating with the existing capacity of each PV system used, one can calculate the total electricity generated by solar energy as a whole. In addition, the demand for potential solar panel installations can be predicted in areas that are suitable for solar energy generation but currently lack such infrastructure.

7. CONCLUSION

This study provided a comprehensive solution to map the solar panel footprints over a large area, aimed at understanding the full picture of solar panel distributions in Hong Kong. In order to prepare for coping with climate change and achieving the United Nations' Sustainable Development Goals, an accurate calculation of the number of solar energy infrastructure is necessary for policymaker and energy agencies to make data-driven decisions regarding infrastructure investments, targeted awareness campaigns, and policy initiatives to pave the “Green Road” for Hong Kong.

REFERENCES

- [1] Chen, Z., Kang, Y., Sun, Z., Wu, F., & Zhang, Q. (2022). Extraction of photovoltaic plants using machine learning methods: a case study of the pilot energy city of Golmud, China. *Remote Sensing*, 14(11), 2697.
- [2] Development Bureau, The Government of the Hong Kong Special Administrative Region. (2023). *Building*. Retrieved from https://portal.csd.gov.hk/geoportal/?lang=en&datasetId=landsd_rcd_1637211194312_35158
- [3] European Commission. (2013). *INSPIRE data specification on land cover – technical guidelines*. Retrieved from https://knowledge-base.inspire.ec.europa.eu/publications/inspire-data-specification-land-cover-technical-guidelines_en
- [4] Electrical and Mechanical Services Department, The Government of the Hong Kong Special Administrative Region. (2022) *Guidance Notes for Solar Photovoltaic (PV) System Installation*. Retrieved from <https://re.emsd.gov.hk/english/files/PVGuidanceNotes.pdf>

- [5] The Green Watt (2023). *Standard Solar Panel Sizes And Wattages (100W-500W Dimensions)*. Retrieved from <https://thegreenwatt.com/standard-solar-panel-sizes-and-wattages-dimensions/>
- [6] Hong Kong Polytechnic University (2021). *Actual Performances of PV Panels in the Local Environment*. Retrieved from https://re.emsd.gov.hk/files/Actual_Performances_of_PV_Panels_in_the_Local_Environment.pdf
- [7] Kausika, B. B., Nijmeijer, D., Reimerink, I., Brouwer, P., & Liem, V. (2021). GeoAI for detection of solar photovoltaic installations in the Netherlands. *Energy and AI*, 6, 100111.
- [8] Lands Department, The Government of the Hong Kong Special Administrative Region. (2023). *Digital Map*. Retrieved from <https://www.landsd.gov.hk/en/survey-mapping/mapping/multi-scale-topographic-mapping/digital-map.html>
- [9] Li, P., Zhang, H., Guo, Z., Lyu, S., Chen, J., Li, W., ... & Yan, J. (2021). Understanding rooftop PV panel semantic segmentation of satellite and aerial images for better using machine learning. *Advances in Applied Energy*, 4, 100057.
- [10] Microsoft Corporation. (2011). *UltraCamEagle - Technical Specifications*. Retrieved from <https://mapafrika.co.za/files/products/1/UltraCamEagle-Specs.pdf>
- [11] Meinhardt (M&E) Ltd (2019). *Executive Summary of Study Report of Photovoltaic (PV) Applications and PV Potential on Building Rooftops in Hong Kong*. Retrieved from https://re.emsd.gov.hk/english/files/2019_Executive_Summary_for_PV_Study_EN.pdf
- [12] Ronneberger, O., Fischer, P., & Brox, T. (2015). U-Net: Convolutional Networks for Biomedical Image Segmentation. *Lecture Notes in Computer Science*, 234–241. https://doi.org/10.1007/978-3-319-24574-4_28
- [13] The Standard. (2023). *Solar panels and canopies blown away by typhoon Saola, no injuries reported*. Retrieved from <https://www.thestandard.com.hk/breaking-news/section/4/207773/Solar-panels-and-canopies-blown-away-by-typhoon-Saola,-no-injuries-reported>
- [14] Wang, J., Chen, X., Jiang, W., Hua, L., Liu, J., & Sui, H. (2023). PVNet: A novel semantic segmentation model for extracting high-quality photovoltaic panels in large-scale systems from high-resolution remote sensing imagery. *International Journal of Applied Earth Observation and Geoinformation*, 119, 103309.
- [15] Wani, M. A., & Mujtaba, T. (2021). Segmentation of satellite images of solar panels using fast deep learning model. *International Journal of Renewable Energy Research (IJRER)*, 11(1), 31-45.

[16] Wu, A. N., & Biljecki, F. (2021). Roofpedia: automatic mapping of green and solar roofs for an open roofscape registry and evaluation of urban sustainability. *Landscape and Urban Planning*, 214, 104167.

[17] Yuan, X., Shi, J., & Gu, L. (2021). A review of deep learning methods for semantic segmentation of remote sensing imagery. *Expert Systems with Applications*, 169, 114417. <https://doi.org/10.1016/j.eswa.2020.114417>

[18] Zhixuhao (2023). Implementation of deep learning framework -- Unet, using Keras. GitHub. <https://github.com/zhixuhao/unet>

BIOGRAPHICAL NOTES

Mr NG Tsz Kin is the Senior Land Surveyor/Remote Sensing Data Analysis of the Lands Department of the Government of the Hong Kong Special Administrative Region. He received his BSc(Hons) degree in Estate Management from the University of Reading in 1993, and MSc degree in Geo-Information Science from the Chinese University of Hong Kong in 2006. He is a professional member of both the Hong Kong Institute of Surveyors (HKIS) and Royal Institution of Chartered Surveyors (RICS).

Mr NG Nok Hang is the former Land Surveyor/Remote Sensing Data Analysis of the Lands Department of the Government of the Hong Kong Special Administrative Region. He received his BSc (Hons) in Geomatics from the Hong Kong Polytechnic University in 2013 and Master degree in National Geo-survey and Public Policy from the Chinese University of Hong Kong in 2016. He is a professional member of both the Hong Kong Institute of Surveyors (HKIS) and Royal Institute of Chartered Surveyors (RICS).

CONTACTS

Mr NG Tsz Kin & Mr NG Nok Hang
Survey and Mapping Office, Lands Department, HKSAR Government
24th floor, North Point Government Offices,
333 Java Road, North Point
HONG KONG
Tel. + 852 2231 3318 / +852 2158 4866
Email: slsrsda@landsd.gov.hk / lsst@landsd.gov.hk